UNPUBLISHED PRELIMINARY DATA

SYMPOSIUM ON QUANTITATIVE SPECTROSCOPY

AND

APPLICATIONS IN SPACE SCIENCE

20-22 March 1963

California Institute of Technology

Pasadena, California

PREPRINT OF PAPER

Radiation Losses From High-Temperature Gas Discharges*

by

Alan C. Kolb
Radiation Division
U. S. Naval Research Laboratory, Washington, D. C.

GPO PRICE $ _____

OTS PRICE(S) $ _____

Hard copy (HC) _2.00_

Microfiche (MF) _.50_

1

NASA CR-50,352

INTRODUCTION

High-temperature spectroscopy is emerging as a subject of considerable interest from several different points of view. In the first place it is important to recognize the very close connection between basic problems in solar and stellar astrophysics and those encountered in diagnosing the properties of laboratory plasmas with electron temperatures in the 10^4 °K-10^7 °K range. In both laboratory and stellar plasmas the emission of radiation can play an important role in determining the over-all energy balance.

In controlled thermonuclear fusion research, the presence of small concentrations (1% or less) of high-Z impurity ions in an otherwise pure deuterium plasma can give rise to an extremely high radiative energy loss rage. Such losses present a serious obstacle to achieving success in various thermonuclear enterprises.

There is also interest in the utilization of high temperature plasmas as light sources, especially in the vacuum ultraviolet. For example, it has been frequently pointed out that the systematic generation of high-excitation spectra of multiply ionized atoms in laboratory plasmas of approximately known density, composition, and electron temperature would greatly aid in the identification of rocket and satellite spectra of the solar corona.

The time-history and absolute intensities of the vacuum ultraviolet emission spectrum can also give valuable information on collisional and radiative processes, i.e., transition probabilities, excitation and recombination cross-sections, ionization rates and the like.

2

In this paper we shall give an account of some numerical calculations of the impurity-radiation losses and cooling of a deuterium plasma produced by high-current electrodeless discharges in low-inductance, single-turn coils (θ-pinches). Electron temperatures in the 10^6 $^\circ$K range have been measured in a number of laboratories from the soft x-ray radiative recombination-bremsstrahlung continuum emitted by such plasmas and it is possible to make a semi-quantitative comparison of the theory with available experimental data.

The present calculations are of a preliminary nature and only serve to indicate the influence of radiative energy losses on the hydromagnetic behavior of the plasma. More detailed hydromagnetic calculations are in progress (McWhirter, Kolb). These are based on a Coronal Plasma model for the radiation in much the same way as has been done earlier[1] for a homogeneous plasma. The new calculations yield the time-dependent intensities of various spectral lines which depend on the time and space variations of temperature and

---

1. Hobbs, G. D., R. W. P. McWhirter, W. G. Griffin and T. J. L. Jones, Proceedings V International Conference on Ionization Phenomena in Gases. Munich p. 1965 (1961)

density. Despite the comparatively high electron densities ($\sim 10^{17}$ cm^{-3}) of these plasmas it is considered that the Coronal model is applicable[2,3,4] because of the high charge of the ions produced at these temperatures ($>10^5$ °K). One goal of the more detailed theory is to compute the time-dependence of the strongest ionic spectral lines for comparison with experiment in order to gain information on the heating mechanisms and the validity of the hydromagnetic theory as applied to the fast magnetic compression of plasmas.

HYDROMAGNETIC EQUATIONS AND HEATING MECHANISMS

The two-fluid (ions and electrons) hydromagnetic θ-pinch equations coded earlier for a digital computer[5,6,7] have been modified to take into account the radiation losses due to the

2. D. R. Bates, A. E. Kingston and R. W. P. McWhirter, Proceedings Royal Society. (London) A <u>267</u>, 297 (1962).

3. R. Wilson, J. Quan. Spect. and Rad. Transfer <u>2</u>, 477 (1962).

4. H. R. Griem, Validity of Local Thermal Equilibrium in Plasma Spectroscopy (to be published in Physical Review).

5. K. Hain, UKAEA report AERE-R3383 Pinch Collapse (1961).

6. K. Hain, G. Hain, K. V. Roberts, J. J. Roberts and W. Köppendörfer, Natursforsch., <u>154</u> 1039 (1960).

7. K. Hain and A. C. Kolb, Nuclear Fusion, 1962 Supplement, Part 2, p. 561.

4

electronic excitation and radiative decay of the lowest
excited states of impurity ions. The radiation cooling
of the electrons is therefore taken into account together
with the joule heating, compressional heating and energy
transport by thermal conduction. The ion temperature is
controlled mainly by compression and electron-ion thermal
relaxation. However, the full non-linear theory also takes
into account shock heating of the ions when it is important
(at high Mach numbers) [7],[8],. For the experimental cases
discussed later the shock structure is determined mainly by
the resistivity since the plasma viscosity is relatively small.
Consequently, the Joule heating rate of the electrons is
greater than the shock heating of ions due to the work done
against viscous stresses. For a pure deuterium plasma, one
therefore expects that the electron temperature will exceed
the ion temperature if the time-scale is less than the ion-electron
energy relaxation time.

In the analysis of stellar spectra one generally employs a
self-consistent model atmosphere analysis which usually includes
the coupled equations of hydrostatic equilibrium and radiative
transport. The fluid aspects of the θ-pinch problem is complicated

7. K. Hain and A. C. Kolb, Nuclear Fusion, 1962 Supplement,
    Part 2, p. 561

8. The importance of shock heating is discussed more fully in
    A. C. Kolb, Comments on the Fast Magnetic Compression of
    Plasmas, Proceedings of the 1962 Univ. of Michigan Summer
    Conf. on Neutron Physics, Boyne Mountain, Mich. (in press)

by the necessity of taking into account the dynamic behavior in the presence of strong magnetic fields. In any case, the hydromagnetic theory described above provides the "model atmosphere" for laboratory astrophysics, in analogy to the more familiar methods of conventional astrophysics.

RADIATION LOSS TERM*

In the so-called corona regime[9], where collisional de-excitation is unimportant, the collisional excitation time of bound states from the ground state of an impurity ion is large compared to the decay time due to spontaneous emission. In that case (which corresponds to the state of affairs in a high-temperature θ-pinch), the radiative power (per radiator) in a single resonance line is given by the collisional exciation rate multiplied by the photon energy.

$$S_{rad} = N_e \langle \sigma_{1n} v \rangle_{av} E_{1n} \tag{1}$$

---

9. G. Elwert, Z Natur f. 7a, 432 (1952)

* The discussion in this section has no new features and is only included to assist in the discussion of the final results.

6

where N_e is the electron number density, σ_{1n} is the cross-section for electronic excitation of the state n from the ground state, $\underline{v}$ is the electron velocity, E_{1n} is the excitation energy measured from the ground state and $\underline{av}$ denotes an average over the electron velocity distribution. Because of the short electron collision times (compared to the experimental times), a Maxwelliam velocity distribution can be assumed. The cross-section can be estimated in various ways[2,4,10,11] and is approximately[3]

$$\sigma_{1n} \approx \frac{\pi\, e^4}{(\frac{1}{2}mv^2)} \frac{f_{1n}}{E_{1n}} \tag{2}$$

where f_{1n} is the usual absorption oscillator strength. The average indicated in (1), using (2), yields

$$S_{rad} \approx \frac{N_e\, 2\, e^4\, f_{1n}}{m} \left(\frac{2\pi m}{k\, T_e}\right)^{1/2} \exp\left(-E_{1n}/k\, T_e\right) \tag{3a}$$

$$\approx 10^{-n}\, \frac{N_e\, f_{1n}}{\sqrt{T^1}} \exp\left(-E_{1n}/T^1\right) \text{erg/ion/cm}^3 \text{ sec,} \tag{3b}$$

10. M. J. Seaton, Ch.11 in "Atomic and Molecular Processes" edited by D. R. Bates (Academic Press, New York, 1962).
11. M. Gryzinski, Phys. Rev. 115, 374 (1959).

where in (3b) T' is the electron temperature expressed in electron volts. One notices that the energy E_{1n} cancels in the coefficient to the exponential term. For this reason the radiation loss rate does not depend strongly on the radiating ionic species. This can be demonstrated numerically by considering oxygen as an example. The energy of the first excited states of the oxygen ions are:

Table 1

Species	E_{12}	Ionization Potential (eV)
OIV	16	77
OV	20	114
OVI	12	138
OVII	573	739
OVIII	653	871

The OIV through OVI spectrum will appear successively for temperatures in the range ~10-30 eV. Since E_{12} is of the order 10-20 eV for all these ions, the power loss depends on the factor $(T^1)^{-1/2} \exp(-E_{12}/T^1)$, which is 0.1 to within a factor two over the indicated range of temperatures, where the various species exist in appreciable numbers according to the model. The situation is similar for other common impurity ions, for plasma temperatures of a few tens of electron volts, since the lowest lying levels usually have an energy of about 10eV. Using estimated f-numbers of a few tenths for these levels, the radiated power is approximately

$$S_{rad} \approx 10^{-19} N_e \text{ erg/impurity ion/cm}^{-3}\text{- sec} \quad (3c)$$

8

at higher temperatures ($\gtrsim$ 200eV), the OVII and OVIII spectra
are strongly excited, but the absolute radiation loss rate is
not much different (within factors of 2 or 3) than given by
(3c) since the characteristic energy of the resonance lines
E_{12} increases as the ionization increases due to the higher
temperature. In making this latter estimate one notes that the
ionization potential and the energies E_{1n} are comparable for
OVII and OVIII-this is not the case for OV etc. (here $E_{12} \ll E_{1n}$)
$n > 2$)*. For these latter species the radiation from the first
excited state dominates because of the large energy gap to the
next level above the first excited state. Therefore, many
OVII and OVIII levels will be excited strongly by electron
collisions, and one would take the effective f-number to be
of the order unity, according to the f-sum rule. Then (3c)
applies also to OVII, OVIII within factors of two at temperatures
of a few hundred eV, which is also of the order of uncertainties
in the magnitude of the excitation cross-section and effective
f-number. If the temperature is high enough ($\gtrsim$300-400eV) and
if the ionization relaxation time $\lesssim$ experimental times, then
even the OVIII lines will begin to disappear as the last remaining
electrons are stripped off and the radiation losses will drop
sharply. This condition has not yet been demonstrated for any
laboratory plasma.

---

* Here n labels the excited states and is not necessarily the
principle quantum number; n increasing with increasing
excitation energy.

Experimental Parameters

The numerical solutions of the hydromagnetic equations discussed here apply to two experiments. One is a relatively fast compression experiment at Jülich, Germany, in which the initial impurity level was established to be about 0.05% in a deuterium plasma[12],[13]. Under these conditions the radiation losses are not expected (using Eqn. 3) to be serious during the experimental times of 1μsec. However, with the addition of 5% (in number density) carbon to the deuterium, the measured electron temperature dropped from 400 eV for a pure plasma to 150 eV. The heating rate was observed to be about 1000 eV/μsec without the addition of carbon.

The other experiment for which calculations have been carried out corresponds to a relatively slow compression, utilizing the megajoule capacitor bank at NRL[14]. With a few percent impurity (mainly oxygen) the discharge is radiation

---

12. P. Bogen, E. Hintz, J. Schlueter, "The Influence of impurities on the Electron Temperature and Soft X-ray Intensity at High Temperatures and Densities," Tagung der Deutchen Physikaleschen Gesellschaft, Stuttgart.(1962)

13. P. Bogen, E. Hintz, J. Schlueter, "Comparison of Theta Pinches with Bias Fields of Different Polarity" Am. Phys. Soc. Div. of Plasma Physics Annual Meeting, Atlantic City, N. J. (Nov. 1962).

14. A. C. Kolb, H. R. Griem, W. H. Lupton, D.T. Phillips, S. A. Ramsden, E. A. McLean, W. R. Faust, M. Swartz, Nuclear Fusion, 1962 Supplement Part 2, p. 553.

10

limited, reaching 300-400 eV for a few microseconds near peak current. With better vacuum conditions (the absolute impurity level is not yet known but is estimated to be of the order 0.1% or less) the electron temperature reaches about 1000 eV. In both the fast and slow experiments, the electron temperature therefore varies by factors of about three, depending on the impurity concentration. The object of these numerical studies is to determine whether the radiation losses by optically-thin resonance lines can qualitatively account for the available observations of radiation limited discharges.

Table 2

Parameters of the NRL and Jülich experiments.

	Jülich	NRL
Coil length	10 cm	180 cm
Initial Plasma radius	1.8 cm	4.4 cm
H_{max}	60 kG	80 kG
Quarter period	1 μsec	15 μsec
Voltage	23 kV	20 kV
Implosion time	0.15 μsec	0.8 μsec
Initial pressure D_2	0.1 Torr	0.02-0.05 Torr

Numerical Results

(A) Julich Experiment

The data was obtained both with an initial trapped reverse field of -1000 G and with a low parallel field of +100 G. The final electron temperatures observed in both cases were comparable.

Figures 1, 2 show the calculated electron temperature on the axis as a function of time. During the initial implosion the rising temperature is not strongly influenced by the addition of carbon since the times are too short to radiate a significant amount of energy, i.e. the Joule heating rate is large compared to the radiation loss rate at lower temperatures when the resistivity is high. However, at later times the radiation loss rate exceeds the heating rate and the electron temperature falls. Also one notices that the radiation losses tend to damp the hydromagnetic oscillations. In Figure 2, the trapped magnetic field on the axis is plotted. With excessive radiation losses from added carbon the resistivity is some five times larger than for a pure plasma so that the internal field decays more rapidly.

The ion temperature for $B_{z\delta} = 100$ G is shown in Figure 3. The radiation losses do not cool ions nearly as much as the electrons since the ion-electron relaxation time is longer than the experimental times with electron densities of the order 10^{17} cm^{-3} at temperatures of a few hundred electron volts.

12

11

The ratio of the electron and ion temperatures (Fig. 4) is greater than unity throughout the discharge if radiation losses are negligible. The Joule losses due to high current densities (up to 350 KA at 0.5μsec) preferentially heat the electrons in this case. However, with 5% carbon, the radiative losses of ~20 megawatts/cm^3 exceed the Joule heating rate of ~7 megawatts/cm^3 and the electrons are cooled. Accordingly, in fast magnetic compression experiments with a few percent impurity, an observed ratio $T_e/T_i < 1$ could be interpreted as preferential electron cooling rather than preferential ion heating.

The calculated radial distribution of the electron temperature and magnetic field near maximum compression for the $B_{zo} = +100$ and -1000 gauss cases are shown in Figs. 5, 6. Here one observes significant differences in the distributions with and without added impurities. The external magnetic field penetrates further into the plasma column if the discharge is radiation limited. In the reverse field case, the field reversal occurs over a few millimeters near the axis and it is interesting to note that a small magnetic probe, with a diameter of a millimeter or two, could not be expected to yield significant information on the existence of a trapped reverse field near current maximum.

The radial position of the maximum current density (or electron density)coincides with the point of field reversal

with $B_{z_0} = -1000$ gauss and is shown in Fig. 7. According to these calculations, the overall dynamic behavior, as observed with a streak camera for instance, should be roughly the same in the two cases. The calculated final electron temperatures of $\sim$450 eV (pure case) and $\sim$140 ev (5% added carbon) correspond closely to the experimental values which indicates that ordinary collisional dissipation at high current densities (described by the transverse Spitzer resistivity) can account for most of the electron heating. One can also conclude that the observed radiation-limited temperature seems to be connected with resonance radiation from CV and CV1 levels with excitation energies between 300 and 400 eV.

The general similarity of the time-dependence of the electron temperatures with a low parallel field (high initial β) and a reverse trapped field shows that a reverse field is not necessary for producing high electron temperatures, as was suspected earlier. In both cases resistive diffusion leads to about the same heating rates. However, with a low parallel trapped field one can expect the end losses to be more important. End losses will be inhibited by closed field lines at the end of the plasma column if there is a reverse trapped field.

In the slow compression case, the heating rate is low (here the current densities are $\sim$70 KA/cm^2) compared to the radiation loss rate even during the implosion (Figs. 8,9).

13

14

Temperature differences of the order three are calculated for pure deuterium and deuterium with 2% added oxygen.

The radiation losses suppress the strong temperature gradients (Fig. 8) due to the converging shock wave which is reflected at the axis.

The radiation losses are mainly due to OV and OVI ions at early times. After the ionization of OVI is complete, the radiation losses will then be small until the temperature rises to about 200 eV, when the 573 eV resonance line of OVII will radiation limit the temperature to ~300 eV. The rapid build-up and decay of the OV radiation is shown in the oscillogram (Fig. 10). After a few microseconds the radiation from OVI will predominate. The qualitative behavior of the observed time-dependence ov OV lines in the discharge is as expected from the numerical calculations.

In general, the observed gross features of θ-pinch discharges can be described by the hydromagnetic theory, including Corona-like radiation effects. However, a detailed comparison between the theory and experiment has not yet been made. Such a comparison would require careful space and time-resolved vacuum ultraviolet measurements of lines from different ions. Such measurements are in progress.

FIGURE CAPTIONS

Fig. 1   Electron temperature on axis with and without added carbon impurity. $B_{zo} = +100$ G. (Julich)

Fig. 2 T_e and B_z on axis. $B_{zo} = +100$ G. (Julich)

Fig. 3   Ion temperature on axis and magnetic field at the wall for $B_{zo} = +100$ G. (Julich)

Fig. 4   Ion-electron temperature ratio on axis with and without added impurity. (Julich)

Fig. 5   Radial temperature and field distributions. $B_{zo} = +100$ G. (Julich).

Fig. 6   Radial temperature and field distributions. $B_{zo} = -100$ G. (Julich).

Fig. 7   Radial motion of the point in the plasma where the internal field changes sign and the density is a maximum. (Julich).

Fig. 8   Electron temperature at the point of maximum density as a function of time with and without oxygen impurities. (NRL).

Fig. 9   Radial distribution of the electron temperature and magnetic field on the axis at the time of maximum compression during the first implosion. (NRL).

Fig.10   Oscillogram of OV 2781 $\overset{\circ}{A}$ as discussed in text. (NRL).
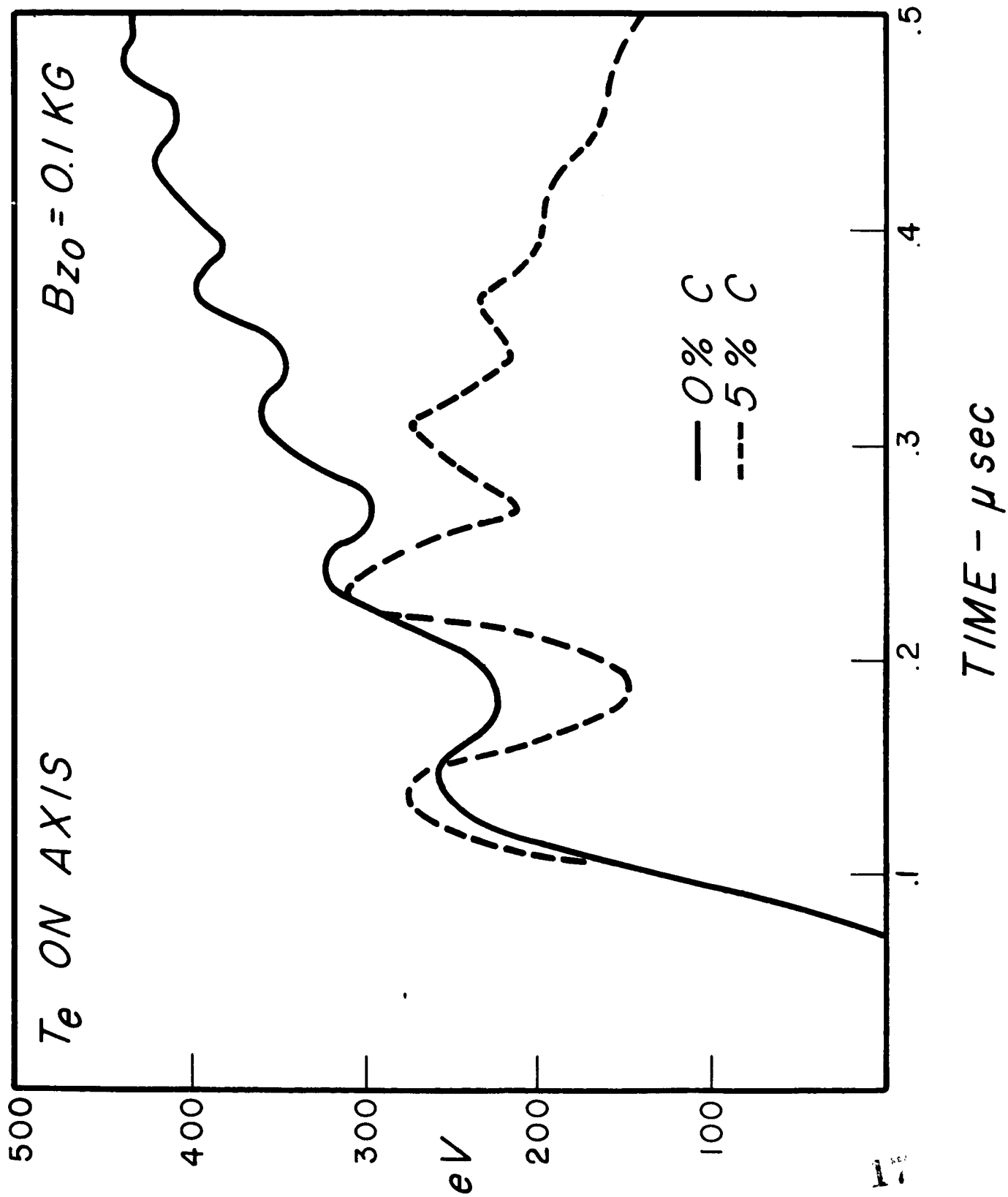
Figure 1

Figure 2

Figure 3
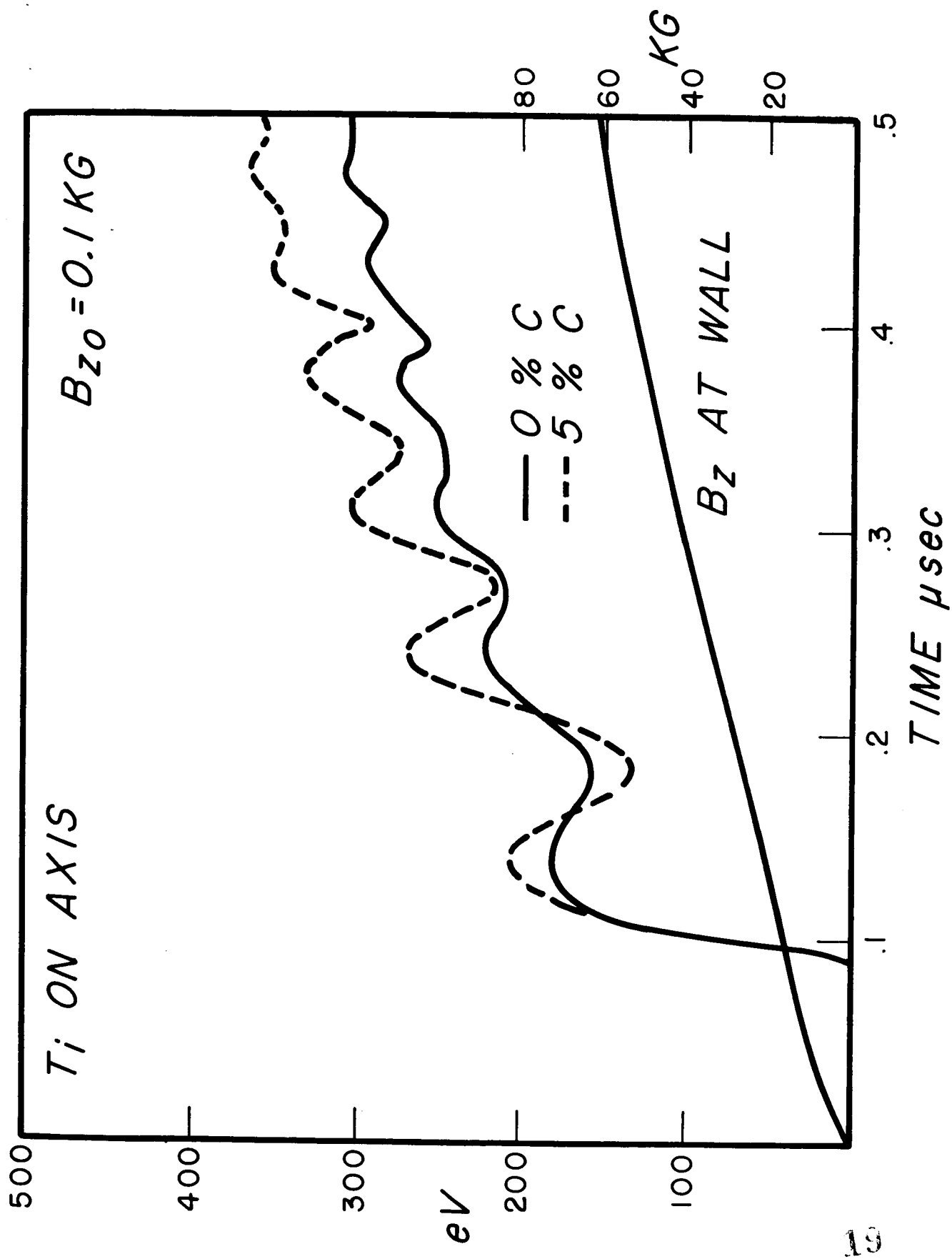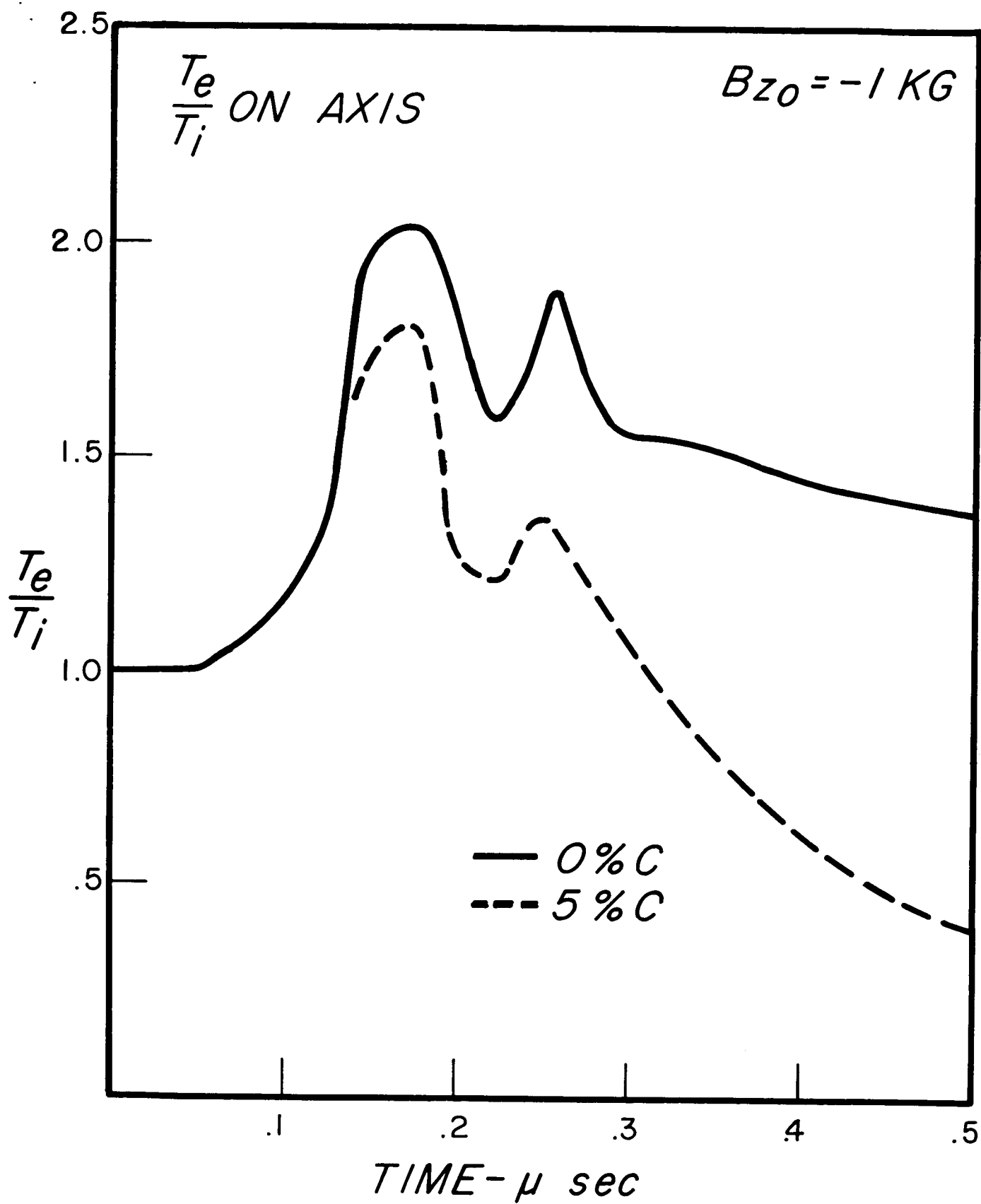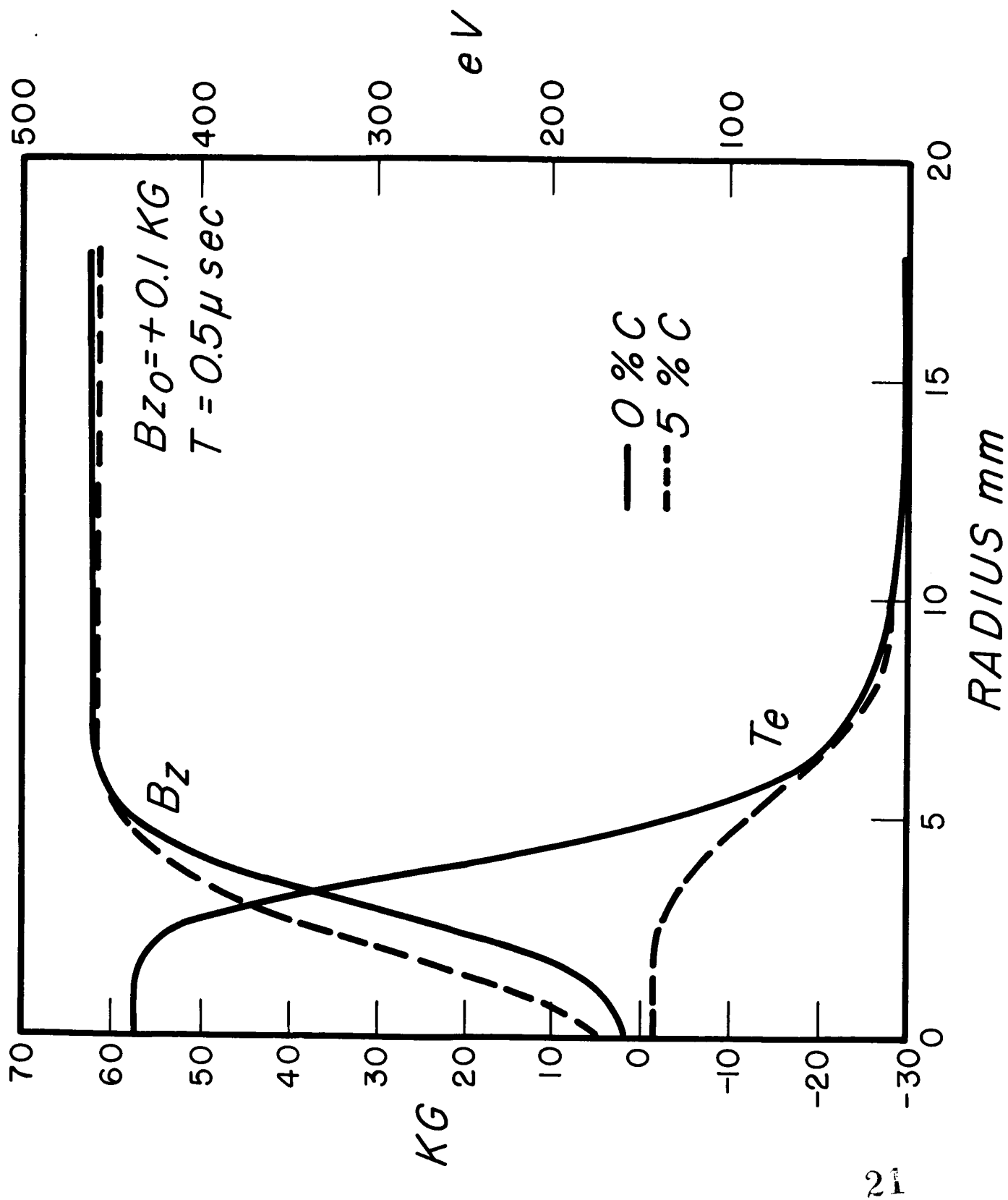
$\frac{T_e}{T_i}$ ON AXIS

$Bz_O = -I KG$

$\frac{T_e}{T_i}$

—— 0%C

--- 5%C

TIME - μ sec

　Figure 4

Figure 5

Figure 6

22

Figure 7

$R(t)$ AT $B_z = 0$

$B_{z0} = -1KG$
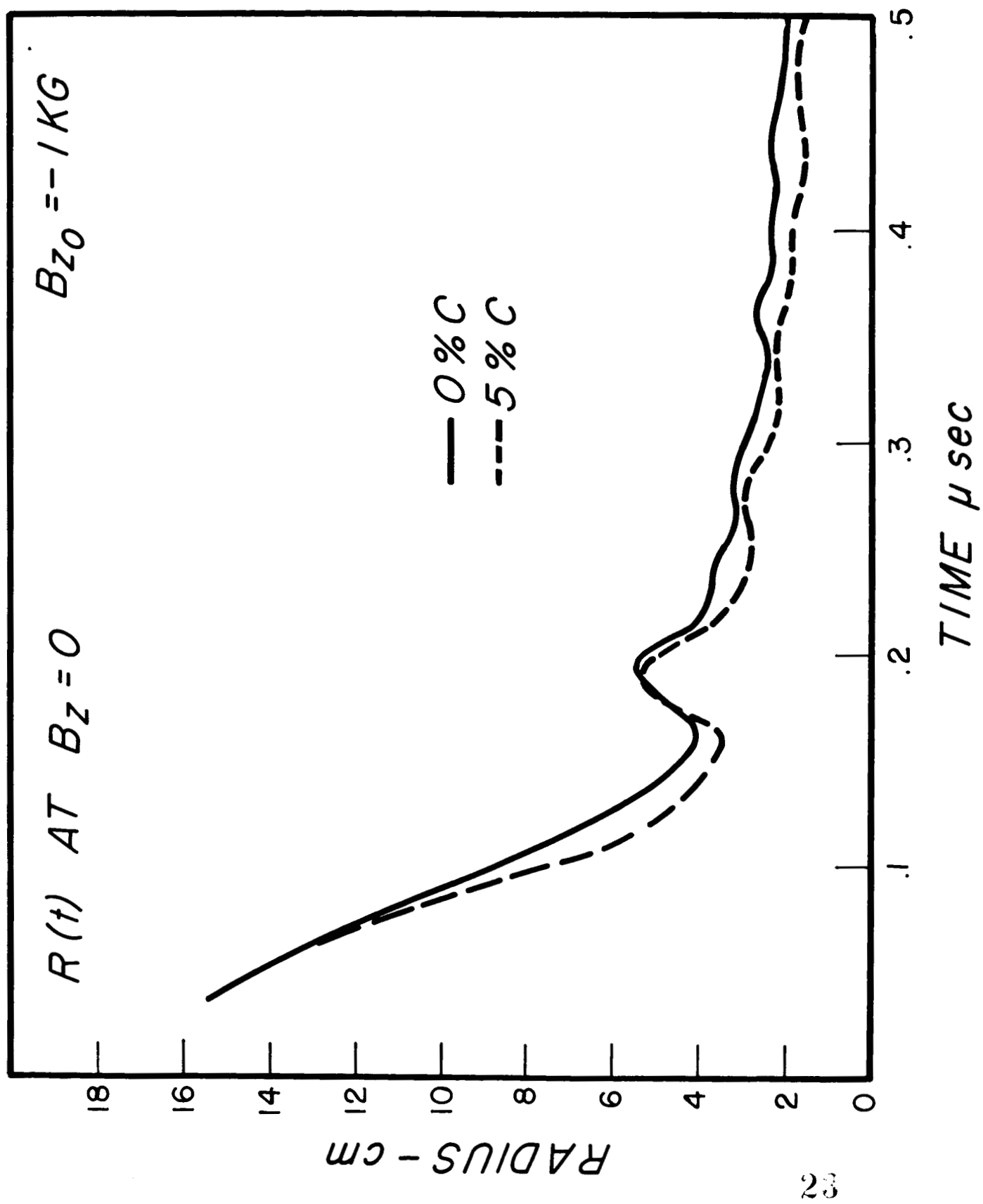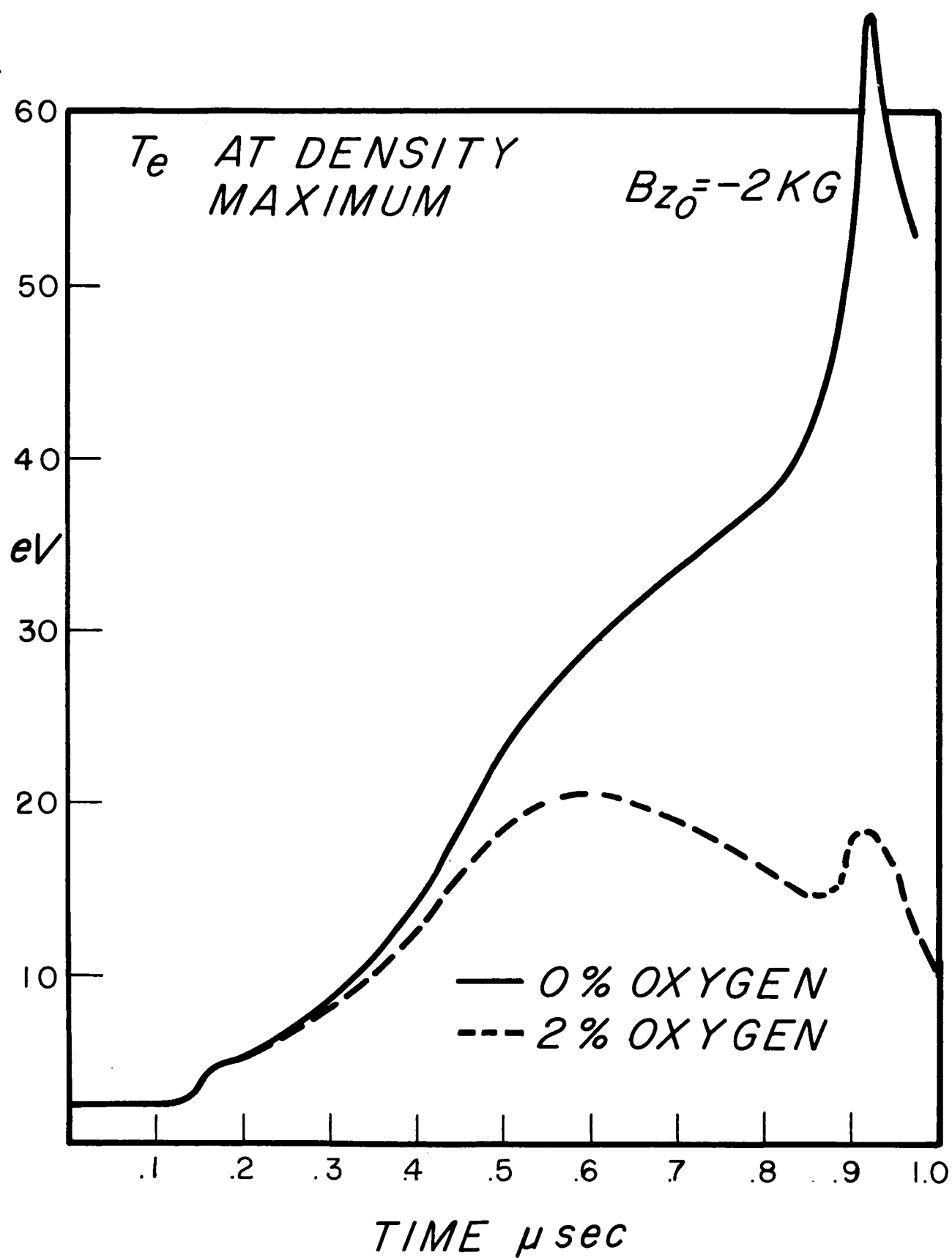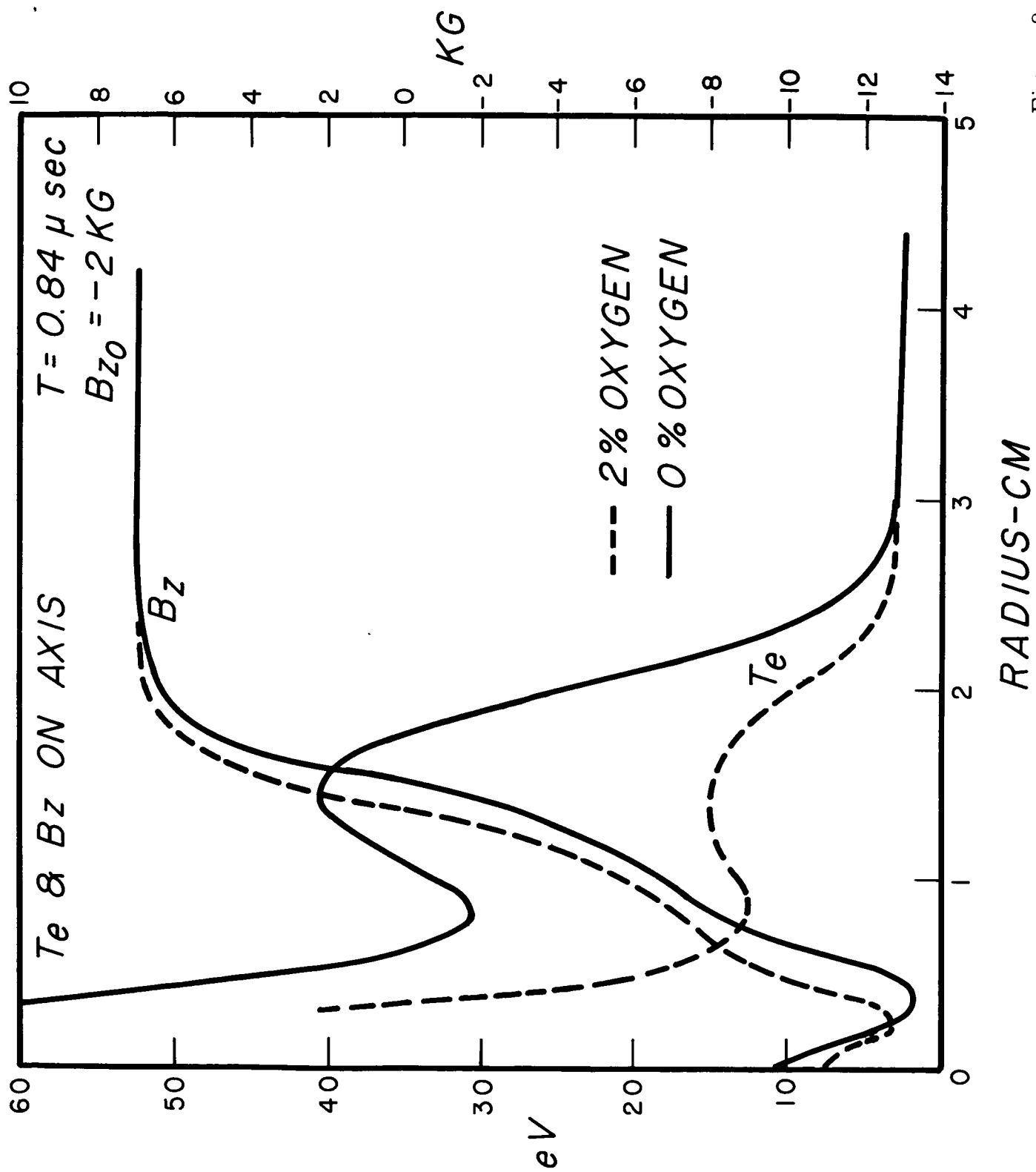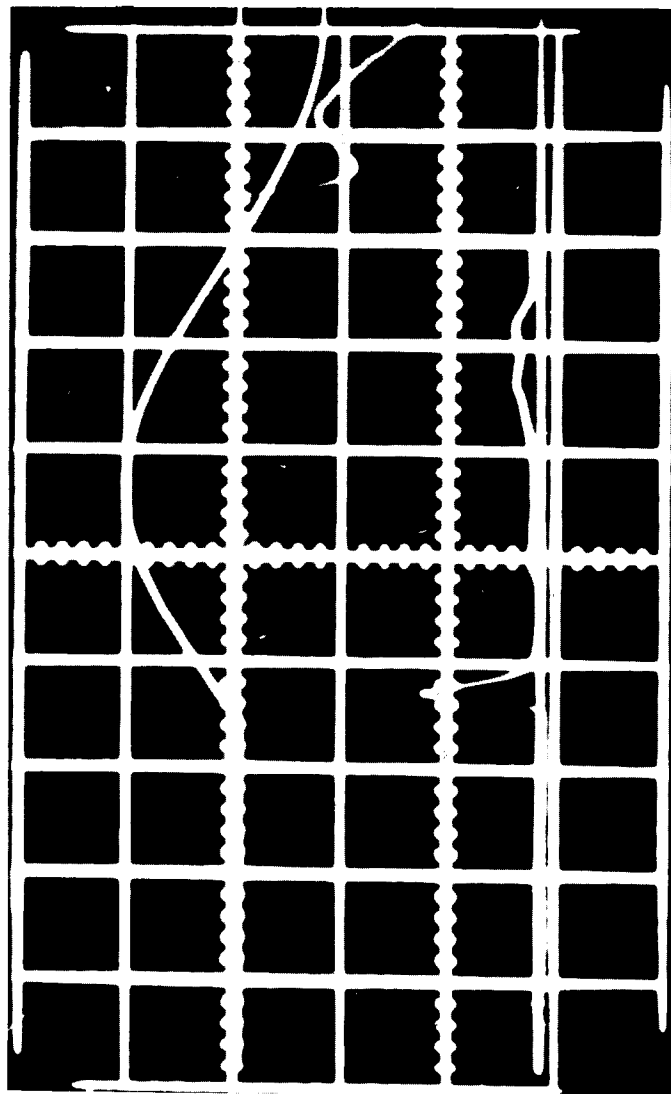
0% C
5% C

TIME μ sec

RADIUS - cm

23
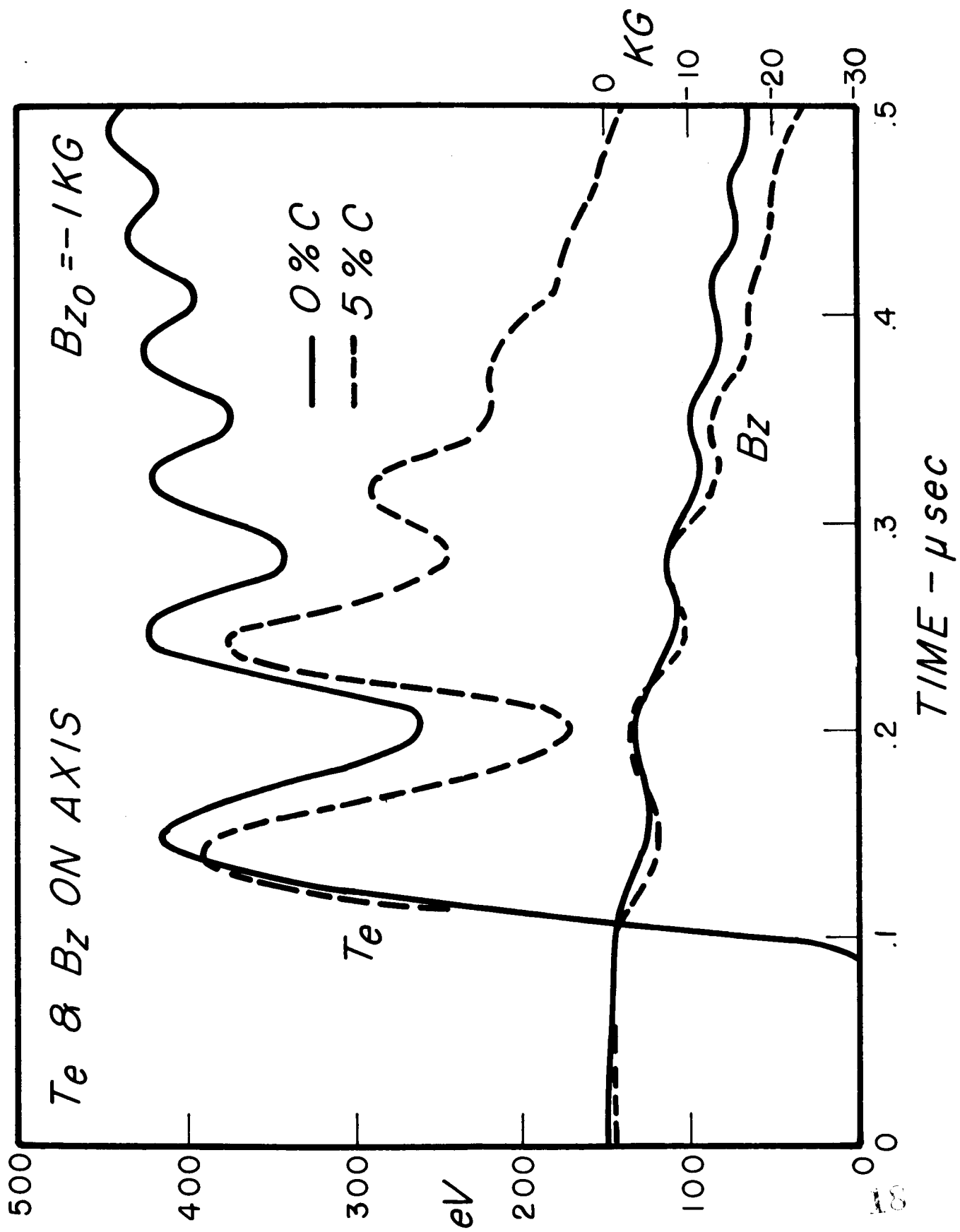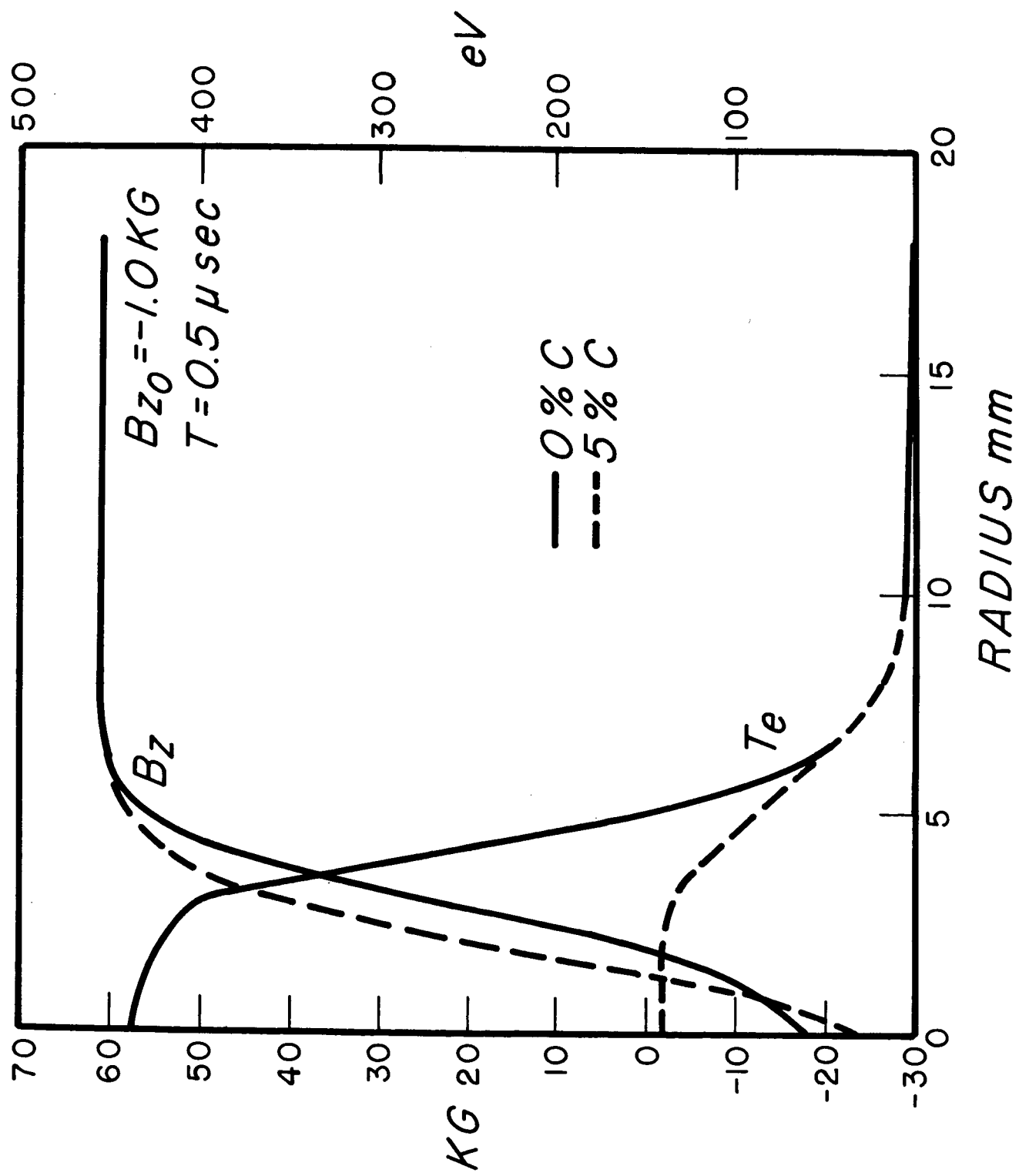
Figure 8

Figure 9

MAIN FIELD

O⊽

5 μ SEC / DIVISION

Figure 10

26